AN ASSESSMENT OF ATMOSPHERICALLY-CORRECTED ASTER EVI FROM GEO GRID

H. Yamamoto [a, *], M. Moriyama [b], and S. Tsuchida [a]

[a] ITRI/AIST, 1-1-1-C2, Umezono, Tsukuba, Japan - (hirokazu.yamamoto,s.tsuchida)@aist.go.jp
[b] Dept. Computer & Information Science, Nagasaki University, 1-14 Bunkyo, Nagasak, Japan - matsu@rsirc.cis.nagasaki-u.ac.jp

Commission VIII, WG VIII/8

KEY WORDS: ASTER/Terra, MODIS/Terra, Enhanced Vegetation Index (EVI), GEO Grid, Atmospheric correction, multi-resolution remote sensing

ABSTRACT:

We developed an on-demand processing service on the GEO Grid system to generate Advanced Spaceborne Thermal Emission and Reflection Radiometer (ASTER) Digital Elevation Model (DEM) and ortho-rectified images. The latest algorithms of radiometric and atmospheric corrections are also supported on this system (Sekiguchi *et al*., 2008). We implemented the MODTRAN3.7-based atmospheric correction for ASTER visible and near Infrared (VNIR) and short wavelength infrared (SWIR) bands on our system. Atmospheric correction algorithm is able to remove Rayleigh scattering, water vapour absorption, and aerosol effects with terrain effects by using ASTER DEM and Moderate Resolution Imaging Spectroradiometer (MODIS) Atmosphere L3 gridded product (MOD08_D3). On the other hand, recent researches confirm the superiority of relationships between Enhanced Vegetation Index (EVI) and biophysical parameters. Yamamoto *et al*. (2010) evaluates three kinds of ASTER EVIs, which include two forms of the two-band EVI with ASTER red and NIR bands but without a blue band and the original, three-band EVI computed with ASTER red/NIR and MODIS blue reflectances generated by the previous GEO Grid system. The atmospheric correction on the previous system does not include the aerosol correction and terrain effect. This research shows the ASTER EVI using new surface reflectance products generated on GEO Grid. MODIS surface reflectance is also generated by the common atmospheric correction, and then ASTER EVIs are compared with MODIS EVI.

1. INTRODUCTION

Satellite remote sensing techniques give the great contributions to the understanding of vegetation dynamics and carbon cycle. Especially, AVHRR/NOAA, Moderate Resolution Imaging Spectroradiometer (MODIS) onboard Terra, and Aqua satellite data have contributed to help the understanding of climate change (e.g. Running, 2008).

Normally, vegetation indices (VIs) are used for the above the researches, and Normalized Difference Vegetation Index (NDVI) is the most popular index, and many researches use this index observed by NOAA AVHRR for understanding historical trend of vegetation dynamics (Los *et al*., 2000). However, it is known that the NDVI has the demerits of atmospheric effects and soil background brightness. And, NDVI has the disadvantage of saturation in high biomass area. The enhanced Vegetation Index (EVI) is an 'optimized' index designed to enhance the vegetation signal with improved sensitivity in high biomass regions and improved vegetation monitoring through a de-coupling of the canopy background signal and a reduction in atmosphere influence. EVI is computed following this equation (Huete *et al*., 2002):

$$EVI = 2.5 \cdot \frac{\rho_{NIR} - \rho_{red}}{\rho_{NIR} + 6.0 \cdot \rho_{red} - 7.5 \cdot \rho_{blue} + 1}, \tag{1}$$

where ρ_{blue}, ρ_{red}, and ρ_{NIR} are the atmospherically corrected reflectance (totally or partially for molecular scattering, and water vapour and ozone absorptions) for the blue, red, and near infrared (NIR) spectral bands, L is the canopy background adjustment factor that addresses nonlinear, differential NIR and red radiant transfer through a canopy, and C_1 and C_2 are the coefficients of the aerosol resistance term, which uses the blue band to correct for aerosol influences in the red band. EVI has mostly been used for assessments of biomass, biophysical properties like leaf area index (LAI), the fraction of Absorbed Photosynthetic Active Radiation (fAPAR) (Gao *et al*., 2000; Huete *et al*., 2002; Zhu *et al*., 2005), Gross Primary Production (GPP) (Sims *et al*., 2006; Ichii *et al*., 2007; Sims *et al*., 2008), and so on. MODIS science team provides both of the NDVI and EVI data set as the MODIS standard product via LPDAAC/NASA. However, the spatial resolution of MODIS EVI is 500m, and the spatial issues between the ground-measurement data and MODIS products should be considered.

Both of Advanced Spaceborne Thermal Emission and Reflection Radiometer (ASTER) (Yamaguchi *et al*., 1998) and MODIS sensor onboard Terra satellite are optical sensors that can observe the wavelength range from visible to thermal, and these sensors have the possibilities of the simultaneous observation. If EVI derived from ASTER visible and near-infrared (VNIR) at 15m resolution can be calculated, it is very useful for many validation researches using ground-based and satellite-based data. However, the ASTER sensor does not have a blue band so that the EVI equation (1) is not simply applicable to ASTER data. Yamamoto *et al*. (2010) evaluated the performance and

* Corresponding author.

compatibility of two-band ASTER EVIs proposed recently, and ASTER EVI using MODIS blue reflectance. However, that atmospheric correction algorithm did not include the aerosol correction.

The MODIS surface reflectance products (MOD09GA, MOD09GQ, MOD09CMG, MOD09A1, MOD09Q1) are usually used for investigation of biophysical parameters using satellite optical sensors, which is processed by the atmospheric correction included aerosol correction algorithm. These products can be obtained via the Land Processes Distributed Active Archive Center (LPDAAC), NASA. On the other hand, the ASTER GEO Grid system (Sekiguchi *et al.*, 2008) can provide the atmospherically corrected ASTER surface reflectance products that include aerosol correction from 2010.

In this research, we evaluate ASTER EVIs using the atmospherically corrected ASTER data from GEO Grid system, and MODIS surface reflectance daily product, which is observed simultaneously with ASTER data.

2. ASTER EVI ON GEO GRID SYSTEM

2.1 Atmospheric correction on GEO Grid system

The GEO Grid system can provide orthorectified calibrated radiance data of ASTER VNIR/SWIR/TIR, Digital Elevation Model by using ASTER nadir- (Band 3N) and backward-looking (Band 3B) bands, atmospherically corrected surface reflectance of ASTER VNIR/SWIR, surface temperature and emissivity derived from ASTER TIR bands. Radiometric re-calibration based on the vicarious calibration is also available for applying to all ASTER bands. Crosstalk correction is also available in ASTER SWIR bands. The GEO Grid users can select various kinds of options for processing.

We adopted the MODTRAN3.7-based (Berk *et al.*, 1987) atmospheric correction algorithms for ASTER VNIR/SWIR bands on GEO Grid system from 2010. This algorithm is able to correct Rayleigh scattering, water vapour absorption, and aerosol effects with terrain effects by using ASTER DEM and MODIS Atmosphere L3 gridded product (MOD08_D3) (Hubanks *et al.*, 2008). Moriyama (2009) shows the detailed description of this algorithm. The atmospheric correction algorithms for VNIR and SWIR bands use the exoatmospheric solar irradiance. The ASTER science team adopts the irradiance model based on World Radiation Centre (WRC) although there are some differences from the other irradiance models, especially in SWIR region. Therefore, we will add the option for selecting the irradiance models on our system in near future.

2.2 Calculation of ASTER EVI

As described previously, the main issue in calculation of the EVI from ASTER data is the fact that the ASTER sensor does not have a blue band. We evaluated three EVI algorithms, which are the MODIS Backup EVI (Didan *et al.*, 2006), the two-band EVI without a blue band (EVI2) (Jiang *et al.*, 2008), and a coupled ASTER-MODIS EVI. More detail explanations of these three EVIs are shown below.

2.2.1 MODIS Backup EVI (EVI_B): Potentially, The EVI is significantly affected by the presence of snow because of high blue reflectance such that EVI values increase largely although NDVI values are reduced. When there are the snow-covered areas, the MODIS VI algorithm switches to a backup EVI equation that is a Soil-Adjusted Vegetation Index (SAVI)-like equation (Huete, 1988), but its coefficients adjusted for this backup index to have nearly the same dynamic range as the EVI (Didan *et al.*, 2006). Since this backup EVI only requires red and NIR reflectances as the inputs, it can directly be computed with ASTER spectral bands without blue band information. The equation takes the form (Didan *et al.*, 2006):

$$EVI_B = 2.5 \cdot \frac{\rho_{ASTER,NIR} - \rho_{ASTER,red}}{\rho_{ASTER,NIR} - \rho_{ASTER,red} + 1} \tag{2}$$

2.2.2 EVI2 - Two-Band EVI (EVI_P): Another two-band EVI, or EVI2, was proposed recently, that equation was derived to theoretically guarantee its equivalency with the original three-band EVI (Jiang *et al.*, 2008). This two-band EVI can also be computed with only ASTER red and NIR bands as below:

$$EVI_P = 2.5 \cdot \frac{\rho_{ASTER,NIR} - \rho_{ASTER,red}}{\rho_{ASTER,NIR} + 2.4 \cdot \rho_{ASTER,red} + 1} \tag{3}$$

2.2.3 Combined ASTER-MODIS EVI (EVI_C): As described above, the ASTER and MODIS sensors onboard the same Terra platform have the possibilities of simultaneous observation. This index uses the MODIS blue band reflectance with the ASTER red and NIR bands to compute the EVI:

$$EVI_C = 2.5 \cdot \frac{\rho_{ASTER,NIR} - \rho_{ASTER,red}}{\rho_{ASTER,NIR} + 6.0 \cdot \rho_{ASTER,red} - 7.5 \cdot \rho_{MODIS,blue} + 1} \tag{4}$$

3. MATERIALS AND METHODS

These three ASTER EVIs were evaluated for the performance and compatibility over a subset of the FLUXNET validation sites (http://www. fluxnet. ornl. gov/), which is covered enough wide range of land cover conditions. Seven land cover types are selected for vegetated and non-vegetated area (Table.1). The acquisition dates of ASTER products were very close to the summer of 2007 or 2008. MODIS daily surface reflectance products (MOD09GA, Collection 5) acquired over these areas simultaneously with ASTER were used by ordering via LPDAAC/NASA in this research. All the ASTER and MODIS scenes were re-projected onto the same geographic projection and re-sampled into the same 15 m grid spacing with the bi-linear method. Nine 1 km-by-1 km extraction sites were manually located on each of these re-projected and re-sampled ASTER-MODIS scene pairs. The 2007 International Geosphere-Biosphere Programme (IGBP) land cover information from the MODIS Land Cover product (MCD12Q1, Collection 5) were used to assure that each of the 1 km-by-1 km extraction sites was the uniform land cover. ASTER images were used to ensure that each extraction site was cloud-free and cloud shadow-free. Firstly, each of three ASTER EVIs was plotted against the MODIS EVI and linear regression was performed to examine overall trends in their relationships. The simple linear model was used based on previous studies (Jiang *et al.*, 2007; Miura *et al.*, 2008) and our preliminary analysis of this dataset:

$$EVI_{ASTER} = \beta_0 + \beta_1 \cdot EVI_{MODIS} + \varepsilon, \quad (5)$$

where EVI_{MODIS} is MODIS EVI, EVI_{ASTER} is EVI_B, EVI_P, or EVI_C, and ε is the unexplained error term. β_0 and β_1 mean intercept and slope derived from linear regression analysis respectively. The overall differences between the ASTER EVIs and MODIS EVI were summarized with root mean square residuals (RMSR):

$$RMSR = \sqrt{\frac{1}{n}\sum_{i=1}^{n}(EVI_{ASTER,i} - EVI'_{ASTER,i})^2}, \quad (6)$$

where n is the sample size and $EVI'_{ASTER,i}$ is the predicted $EVI_{ASTER,i}$ by the derived linear regression model from the first analysis. When we compare the ASTER and MODIS EVI, the scaling uncertainty should be considered. Wolfe *et al.* (2002) shows the triangular spatial response function along with cross track scanning as the MODIS Point Spread Function (PSF). This research also used this PSF for each inter-comparison.

Land Cover Type	Longitude, Latitude [Decimal Degrees]	Image Acquisition Date
Evergreen Needle-leaf forest	N40.033, W105.546	2007.8.8
Evergreen Broad-leaf forest	S11.412, W55.325	2008.7.26
Deciduous Needle-leaf forest	N62.241, E129.651	2008.6.2
Deciduous Broad-leaf forest	N39.914, W74.596	2007.6.9
Croplands	N44.722, W93.089	2007.6.20
Barren or sparsely vegetated	N33.817, W116.373	2007.9.12
Urban and built-up	N39.659, W105.013	2007.9.25

Table 1. FLUXNET sites used in ASTER and MODIS EVI compatibility analysis.

4. RESULTS AND DISCUSSION

Figure 1. shows the scatterplots of MODIS original EVI vs. EVI_B, EVI_P, and EVI_C in this study with the scatterplots shown in Yamamoto *et al.* (2010). The differences between Yamamoto *et al.* (2010) and this study are the following two points.

1. Atmospheric correction algorithm applied in Yamamoto *et al.* (2010) did not include the aerosol correction although the same algorithm is applied to both of ASTER and MODIS data.
2. Atmospheric correction algorithm applied in this study is different from the algorithm used in MOD09GA although this algorithm includes the aerosol correction with terrain effect correction.

On the whole, the correlation is worse than the previous research, but the coefficients themselves are not bad, which show greater than 0.96. Especially, the characteristics of EVIC in this study are lower slope (0.896) and correlation coefficient (0.960) than other two-band EVIs. This result indicates that there is possibility of the effect of MODIS blue reflectance in MOD09GA. Originally, it is easy for the blue reflectance to be affected by the atmospheric condition. Therefore, the MODIS surface reflectance should be processed by the ASTER atmospheric correction algorithm on the GEO Grid system. MOD09GA blue reflectance pixels need to be also evaluated by the quality assessment flags.

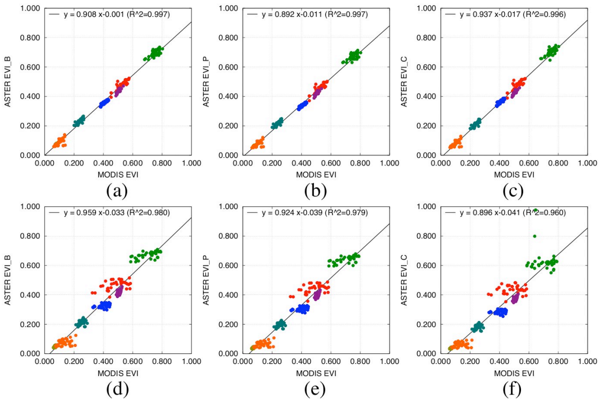

Figure 1. Upper three scatterplots show MODIS original EVI vs. EVI_B (a), EVI_P (b), and EVI_C (c) in Yamamoto *et al.* (2010). Lower three scatterplots are MODIS original EVI vs. EVI_B (d), EVI_P (e), and EVI_C (f) in this study.

Figure 2. shows the comparison between MODIS EVI image and ASTER EVIC image applied the linear regression results shown in Figure 1. (f), which are the same place of cropland. As this figure shows, MODIS EVI has the possibilities of the gaps between ground measurement data. On the other hand, ASTER EVI can discriminate more detailed distributions for the croplands. This means that 15m ASTER EVIs are very useful for the validation researches because the long-term and finer resolution of ASTER data since 2000 can be used.

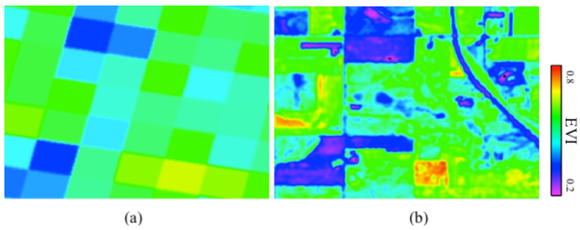

Figure 2. The comparison between MODIS EVI (a) and ASTER EVI_C in this study (b). Both of images are the same place of the cropland located at Rosemount of Minnesota in USA.

Table 2. compares the RMSR values among the ASTER EVIs in the previous and this study. RMSR of EVI_P (0.023) was smallest in the previous study, but almost same as EVI_B (0.029) and EVI_C (0.028). On the other hand, both of EVI_B (0.044) and EVI_P (0.044) were smaller than EVI_C (0.062) in this study, and the difference between two-band EVIs and EVI_C is large. These show the same results as the above-mentioned correlations. EVI_C depends on the accuracy of MODIS blue reflectance, and more validation works for ASTER atmospheric correction algorithm on GEO Grid system are also needed.

	EVI_B	EVI_P	EVI_C
ASTER EVI using atmospherically corrected surface reflectances in Yamamoto *et al.* (2010)	0.029	0.023	0.028
ASTER EVI using atmospherically corrected surface reflectances in this study	0.044	0.044	0.062

Table 2. Root mean square residuals (RMSR) of each ASTER EVIs

5. CONCLUSIONS AND FUTURE WORK

MODIS EVI derived from the daily MODIS surface reflectance products are used in many biophysical researches, but the spatial gap between MODIS EVI and ground-based data is important issue that should be solved. ASTER EVI is very useful for validation research in biophysical parameters because ASTER is onboard the same platform, Terra satellite. This paper evaluated the two-band ASTER EVIs (EVI_B and EVI_P) and three-band EVI (EVI_C), which were derived from the atmospherically corrected ASTER surface reflectance provided by the GEO Grid system and MOD09GA blue reflectance in provided by LPDAAC/NASA. All ASTER EVIs were evaluated by comparing their values to those of MODIS EVI over the seven FLUXNET sites covering a wide range of land cover types. The following points are concluded in this study.

1. Two-band ASTER EVIs (EVI_B and EVI_P) have mostly same accuracy, and this accuracy depends on the ASTER atmospheric correction algorithm. Therefore, more validation of ASTER surface reflectances is needed.
2. Three-band ASTER EVI (EVI_C) using MOD09GA blue reflectance also depends on the pixel quality of blue reflectance, and the MOD09GA blue reflectance pixels should be evaluated by the quality assessment flags.
3. If the same algorithm as the ASTER atmospheric correction corrects the MODIS blue reflectance, there is the possibility of more accurate MODIS equivalent ASTER EVI by using MODIS blue reflectance.

In the case of ASTER EVI using the current ASTER surface reflectances and MOD09GA products, we will validate the atmospherically corrected ASTER surface reflectances on GEO Grid system by ground-based data and/or the inter-comparison of various satellite data firstly, and then low or poor quality pixels should be removed by quality assessment flags of MOD09GA products. Furthermore, the validation will be conducted over more various land cover types. On the other hand, the simulation experiments under various atmospheric conditions are also planned. The current ASTER atmospheric correction algorithm that is able to apply to the MODIS L1B products (MOD02HKM) will be implemented to the GEO Grid system in near future.

ACKNOWLEDGEMENTS

This research used ASTER Data beta processed by the AIST GEO Grid from ASTER Data owned by the Ministry of Economy, Trade and Industry.

REFERENCES

Berk, A., Bernstein, L.S., and Robertson, D.C., 1989. MODTRAN: A moderate resolution model for LOWTRAN 7. *AFGL_TR-89- 0122, U. S. Air Force Geophysics Laboratory,* Hanscom Air Force Base, MA.

Didan, K. and Huete, A., 2006. MODIS Vegetation Index Product Series Collection 5 Change Summary. http://modis-250m.nascom.nasa.gov/QA_WWW/forPage/MOD13_VI_C5_Changes_Document_06_28_06.pdf (accessed 8 Nov. 2009)

Gao, X., Huete, A.R., Ni, W., and Miura, T., 2000. Optical-biophysical relationships of vegetation spectra without background contamination. *Remote Sensing of Environment*, 74(3), pp. 609-620.

Hubanks, P.A., King, M.D., Platnick, S.A., and Pincus, R.A, 2008. MODIS Atmosphere L3 Gridded Product Algorithm Theoretical Basis Document. *Algorithm Theoretical Basis Document ATBD-MOD*, 2(3).

Huete, A.R., 1988. A soil-adjusted vegetation index (SAVI). *Remote Sensing of Environment*, 25(3), pp. 295-309.

Huete, A. Didan, K. Miura, T. Rodriguez, EP Gao, X. and Ferreira, LG, 2002. Overview of the radiometric and biophysical performance of the MODIS vegetation indices. *Remote Sensing of Environment*, 83(1-2), pp. 195-213.

Ichii, K.; Hashimoto, H., White, M., Potter, C., Hutyra, L., Huete, A., Mynenu, R., and Nemani, R., 2007. Constraining rooting depths in tropical rainforests using satellite data and ecosystem modelling for accurate simulation of gross primary production seasonality. *Global Change Biology*, 13, pp. 67-77.

Jiang, Z., Huete, A., Kim, Y., and Didan, K., 2007. 2-band enhanced vegetation index without a blue band and its application to AVHRR data. *Proceedings of SPIE*, 6679, pp. 667905–1–667905–9.

Jiang, Z., Huete, A., Didan, K., and Miura, T., 2008. Development of a two-band enhanced vegetation index without a blue band. *Remote Sensing of Environment*, 112(10), pp. 3833--3845.

Los, S.O., Collatz, G.J., Sellers, P.J., Malmstrom, C.M., Pollack, N.H., DeFries, R.S., Bounoua, L., Parris, M.T., Tucker, C.J., and Dazlich, D.A., 2000. A global 9-yr biophysical land surface dataset from NOAA AVHRR data. *Journal of Hydrometeorology*, 1(2), pp. 183-199.

Miura, T., Yoshioka, H., Fujiwara, K., and Yamamoto, H., 2008. Inter-Comparison of ASTER and MODIS Surface Reflectance and Vegetation Index Products for Synergistic Applications to Natural Resource Monitoring. *Sensors*, 8, pp. 2480–2499.

Moriya, M., 2009, Error analysis of the DEM–employed atmospheric and terrain effect correction scheme, *Proceeding of the 47th Autumn Conference of the Remote Sensing Society of Japan*, pp. 11-12 (in Japanese).

Running, S., 2008. CLIMATE CHANGE: Ecosystem Disturbance, Carbon, and Climate. *Science*, 321(5889), pp. 652-653.

Sekiguchi, S., Tanaka, Y., Kojima, I., Yamamoto, N., Yokoyama, S., Tanimura, Y., Nakamura, R., Iwao, K., and Tsuchida, S., 2008. Design Principles and IT Overviews of the GEO Grid. *IEEE Systems Journal*, 2(3), pp. 374-389.

Sims, D., Rahman, A., Cordova, V., El-Masri, B., Baldocchi, D., Flanagan, L., Goldstein, A., Hollinger, D., Misson, L., Monson, R., Oechel, W., Schmid, H., Wofsy, S., and Xu, L., 2006. On the use of MODIS EVI to assess gross primary productivity of North American ecosystems. *Journal of Geophysical Research*, 111, G04015.

Sims, D.A., Rahman, A.F., Cordova, V.D., El-Masri, B.Z., Baldocchi, D.D., Bolstad, P.V., and Flanagan, L.B., 2008. A new model of gross primary productivity for North American ecosystems based solely on the enhanced vegetation index and land surface temperature from MODIS. *Remote Sensing of Environment*, 112(4), pp. 1633-1646.

Yamaguchi, Y., Kahle, A., Tsu, H., Kawakami, T., and Pniel, M., 1998. Overview of Advanced Spaceborne Thermal Emission and ReflectionRadiometer (ASTER). *IEEE Transactions on Geoscience and Remote Sensing*, 36(4), pp. 1062-1071.

Yamamoto, H., Miua, T., and Tsuchida S., 2010. An Evaluation of ASTER Enhanced Vegetation Index (EVI) Products from GEO Grid for Synergistic Applications with MODIS: A Preliminary Study. *Remote Sensing,* (submitted).

Wolfe, R.E., Nishihama, M., Fleig, A.J., Kuyper, J.A. , Roy, D.P., Storey, J.C., and Patt, F.S., 2002. Achieving sub-pixel geolocation accuracy in support of MODIS land science. *Remote Sensing of Environment*, 83(1-2), pp. 31-49.